Yukawa Institute Kyoto

YITP-98-69
October 1998

Non-axial Octupole Deformations of $N = Z$ Nuclei in $A \sim 60 - 80$ Mass Region *

M. Matsuo

Yukawa Institute for Theoretical Physics, Kyoto University, Kyoto 606-8502, Japan

S. Takami and K. Yabana

Graduate School of Science and Technology, Niigata University, Niigata 950-2101, Japan

arXiv:nucl-th/9810067v1 26 Oct 1998

Abstract

By performing a fully three dimensional Hartree-Fock calculation with use of the Skyrm forces, we demonstrate possibility of exotic deformations violating both the reflection and the axial symmetries of $N = Z$ nuclei in $A \sim 60 - 80$ mass region. The Y_{32} tetrahedral shape predicted in excited ^{80}Zr arises from a shell gap at $N, Z = 40$ which is enhanced for the tetrahedron deformation. Softness toward the Y_{33} triangular deformation of the oblate state in ^{68}Se is also predicted.

*A talk presented by M.M. at *Nuclear Structure '98*, Gatlinburg, August 10-15, 1998

1 Introduction

Octupole deformations that violate the reflection symmetry have attracted many attentions recently in studies of nuclear structure[1]. Although axial octupole deformation is well established in actinides and in neutron rich Xe and Ba region, there seems no experimental evidence of more exotic shapes that violate both the reflection and the axial symmetries, except for light alpha-clustering nuclei such as ^{12}C [2].

Non-axial octupole deformations have been predicted theoretically for actinides [3] and in superdeformed nuclei [4, 5]. Instead we point out possibility of the non-axial octupole shapes in $N = Z$ $A \sim 60-80$ region of the nuclear chart [6, 7]. For $N = Z$ nuclei the deformation driving shell effects which arise from both protons and neutrons cooperate coherently. The shell effect is indeed large in this mass region as is illustrated by the prolate-oblate shape coexistence in Kr and Se isotopes [8] and the sudden onset of large prolate deformation for $N, Z \approx 38 - 40$ [9]. Furthermore octupole instability due to the single-particle structure in nuclear mean-field is predicted for $N, Z \sim 34$ (in addition to $56, 90, 134$) [10, 11] for which the coupling between $g_{9/2}$ and $p_{3/2}$ orbits are mostly responsible.

It is found recently that the shell structures plays important roles for aggregates of metallic atoms (metal clusters). In this system the mean-field for the valence electrons resembles with the nuclear mean-field except for its effectively zero ls potential [12]. Non-axial octupole deformatios seem to be one of the dominant deformations in this system as demonstrated by means of schematic models [13, 14] and more recent mean-field calculations [15, 16]. In particular, the tetrahedron shape or the Y_{32} deformation is predicted to be stable because of the shell gaps generated at $N_{electron} = 40, 70, 112, 156$ [13, 15, 16]. In this paper, we will show that the tetrahedron shape is expected in the nucleus ^{80}Zr with $N = Z = 40$, being in parallel with the metal cluster system in spite of the difference in the ls potential and the pairing correlation present in nuclei. Furthermore, non-axial octupole deformations besides Y_{32} are important deformation modes in $N = Z$ nuclei in $A \sim 60 - 80$ mass region. See also the previous publication [6].

2 A fully three dimensional Hartree-Fock calculation

For investigating non-axial reflection asymmetric deformations by means of the mean-field theory, we have to exclude any symmetry assumptions on nuclear deformations. Furthermore, it is important to use a description which allows arbitrary deformation when we search unknown shapes. From this view point, we adopt the Hartree-Fock method and perform a fully three dimensional calculation using the Cartesian mesh representation without any requirements on nuclear shapes and its symmetries. The Skyrm force is used as the effective nucleon-nucleon force. The pairing correlation is treated by means of the BCS method for the seniority force with a cutoff of the single-particle orbits, which is chosen the same as Ref. [17, 18]. The imaginary time method is used for the iteration procedure [19]. Thus the basic formulation is in parallel with that of Ref.[17], except for the symmetry treatment (they assumed the reflection symmetries) and calculational details. A new code has been developed independently so that it can also include the parity projection and full variation after projection[20]. The parity projected Hartree-Fock with Skyrm force, but without BCS treatment, has been applied to light nuclei[20] (but not to the present investigation).

For the results presented below, we use the 3D mesh which are enclosed by a sphere of radius $R = 13$ fm, and the mesh width of 1 fm. The parameter set of SIII [21] is used for the Skyrm force in most calculations while SkM* [22] is also employed for comparison. Concerning the pairing force, we use $G_p = 16.5/(11 + Z)$ MeV for protons as given in Ref. [17]. For neutrons, we use $G_n = 16.5/(11 + N)$ MeV [23] since it is natural to take the same value as protons for $N = Z$ nuclei. In order to search not only the ground state but also local minimum states, we performed different runs of iterations starting with different initial conditions. To characterize deformation of the obtained solutions, we use the mass multipole moments,

$$\alpha_{lm} \equiv \frac{4\pi \langle \Phi | \sum_i^A r_i^l X_{lm}(i) | \Phi \rangle}{3AR^l}, (m = -l, \cdots, l), \tag{1}$$

where A is the mass number and $R = 1.2A^{1/3}$ fm. Here X_{lm} is a real basis of the spherical harmonics,

$$\begin{aligned} X_{l0} &= Y_{l0}, \\ X_{l|m|} &= \frac{1}{\sqrt{2}}(Y_{l-|m|} + Y^*_{l-|m|}), \\ X_{l-|m|} &= \frac{-i}{\sqrt{2}}(Y_{l|m|} - Y^*_{l|m|}), \end{aligned} \tag{2}$$

where the quantization axis is chosen as the largest and smallest principal inertia axes for prolate and oblate solutions, respectively. We put the constraints $\alpha_{1m} = 0 (m = -1, 0, 1)$ for the center of mass, and $\alpha_{2m} = 0 (m = -2, -1, 1)$ for the principal axes. This is done by adding the constraining fields $-\lambda_{lm} r^l X_{lm}$ to the mean field, where the constraining Lagrange multipliers are determined so that the constraints are satisfied in each iteration step[20].

For the quadrupole moment, we use ordinary (β, γ) notation, i.e., $\alpha_{20} = \beta \cos\gamma, \alpha_{22} = \beta \sin\gamma$, mapped in the $\beta > 0, 0 < \gamma < \pi/3$ section. To represent magnitude of the octupole deformation, we define

$$\beta_3 \equiv (\sum_{m=-3}^{3} \alpha_{3m}^2)^{\frac{1}{2}}, \qquad \beta_{3m} \equiv (\alpha_{3m}^2 + \alpha_{3-m}^2)^{\frac{1}{2}} \qquad (m = 0, 1, 2, 3). \tag{3}$$

3 Shapes of ground and local minimum states

The HF ground states and local minimum solutions for the even-even nuclei ^{64}Ge, ^{68}Se, ^{72}Kr, ^{76}Sr and ^{80}Zr are listed in Table 1. The result is essentially the same as the previous calculation [6] while the convergence of the HF iteration is taken care of more carefully in the present calculation. It is noted that many of these nuclei have local minimum solutions with low excitation energy, suggesting presence of shape coexisting excited states. The ground state shape changes from the triaxial (^{64}Ge), the oblate (^{68}Se,^{72}Kr), to the strong prolate shape (^{76}Sr,^{80}Zr) as N, Z increases. This is consistent with the experimental trends [9, 24, 25].

The reflection asymmetric solutions with non-zero octupole deformation ($\beta_3 > 0$) are obtained as the ground state of ^{68}Se, and as the shape coexisting excited states in ^{76}Sr and ^{80}Zr. These solutions *violate*

Table 1: The ground and local minimum HF solutions obtained with the SIII force. The number in the first line is the excitation energy in MeV measured from the ground state solution. The second and the third line list the quadrupole and octupole deformations of the solutions.

	Oblate $\beta > 0,\ 30^\circ < \gamma \leq 60^\circ$	$\beta = 0$	Prolate $\beta > 0,\ 0^\circ \leq \gamma \leq 30^\circ$
^{64}Ge			g.s. $\beta, \gamma = 0.28, 25^\circ$ (triaxial) $\beta_3 = 0.00$
^{68}Se	g.s. $\beta, \gamma = 0.28, 60^\circ$ $\beta_3 = \beta_{33} = 0.14$		0.25 $\beta, \gamma = 0.25, 0^\circ$ $\beta_3 = 0.00$
^{72}Kr	g.s. $\beta, \gamma = 0.35, 60^\circ$ $\beta_3 = 0.00$		1.47 $\beta, \gamma = 0.40, 0^\circ$ $\beta_3 = 0.00$
^{76}Sr	2.72 $\beta, \gamma = 0.14, 60^\circ$ $\beta_3 = 0.13, \beta_{32} = 0.12$		g.s. $\beta, \gamma = 0.50, 0^\circ$ $\beta_3 = 0.00$
^{80}Zr	1.56 $\beta, \gamma = 0.19, 60^\circ$ $\beta_3 = 0.00$	0.96 $\beta, \gamma = 0.00, 0^\circ$ $\beta_3 = \beta_{32} = 0.23$	g.s. $\beta, \gamma = 0.51, 0^\circ$ $\beta_3 = 0.00$

not only the reflection symmetry but also the axial one. The ^{68}Se ground state has finte Y_{33} deformation ($\beta_{33} = 0.14$) together with oblate quadrupole deformation. The density profile shows a triangular shape, as seen in Fig.1. In ^{80}Zr, the first local minimum solution with the excitation energy of 0.96 MeV has large Y_{32} deformation ($\beta_{32} = 0.23$) whereas the solution has no quadrupole deformation. It has a tetrahedral shape as shown in Fig. 1. Although this solution violates both the reflection and the axial symmetry, the tetrahedral symmetry (T_d) of the point group emerges as a spontaneous symmetry. Indeed the calculated single-particle energy spectrum shows a four-fold degeneracy which is a characteristic feature of the Fermion mean-field with the T_d symmetry [3] (See also Fig.3(c)).

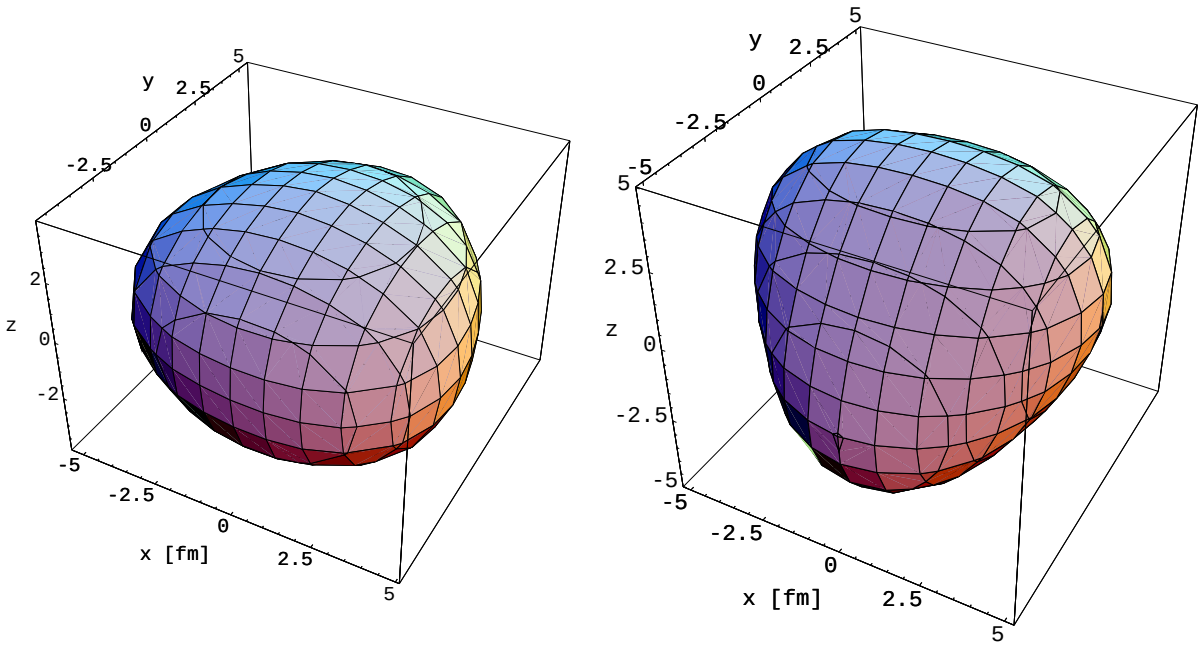

Figure 1: The density contour surface at the half central density for the triangular ground state solution in ^{68}Se (left), and the tetrahedral first local minmum solution in ^{80}Zr (right), listed in Table 1 obtained with the SIII force.

4 Non-axial octupole deformations

Potential energy curves

To evaluate softness of the obtained solutions toward the octupole deformations, we calculate the potential energy curve as a function of the deformation parameters α_{3m} for all the independent components $m = 0, 1, 2, 3$ of octupole deformations by means of the constraint Hartree-Fock calculation. For this calculation, we introduce additional nine constraints for the quadrupole deformation α_{20}, α_{22} (equivalent to β, γ) and the octupole deformations $\alpha_{3m}(m = -3, .., 3)$. The values of β, γ is fixed to the ones of a HF solution under consideration, and one of $\alpha_{3m}(m = 0, 1, 2, 3)$ is varied while other α_{3m}'s are fixed to zero. The calculated potential energy curve is plotted in Fig.2.

Tetrahedron shape and associated shell gap in ^{80}Zr

The tetrahedral solution in ^{80}Zr corresponds to the minimum at $\alpha_{32} = 0.23$ of the α_{32} potential energy curve with the spherical constraint ($\beta = 0$). The energy gain due to the tetrahedron deformation or

Figure 2: Potential energy curve as a function of the octupole deformation $\alpha_{3m} (m = 0, 1, 2, 3)$ associated with the ground and local minimum solutions listed in Table 1.

equivalently the energy difference between the minimum at $\alpha_{32} = 0.23$ relative to $\alpha_{32} = 0$ is as large as 0.70 MeV. It is noted that the potential energy curves for $\alpha_{3m}(m = 0, 1, 3)$ do not show such deep minimum. The reason of this can be seen in the single-particle energy diagram, Fig.3, plotted as a function of the octupole deformations α_{3m}. Figure 3 indicates that the single-particle energy spectrum accompanies a large gap at $N, Z = 40$ which increases as increasing the tetrahedral deformation α_{32} while the other octupole deformations $m = 0, 1, 3$ do not have this feature. This is the gap specific to the tetrahedron deformation, and presence of such gap is due to the high symmetry (the T_d symmetry of the point group) [13]. Note that the tetrahedron shell gap at particle number 40 is found also in the metal cluster systems [16] for which there is no ls potential. Figure 3 indicates that the tetrahedron shell gap emerges even under influence of the large ls term in nuclear potential. It is also noted that the tetrahedron minima is obtained with including the pairing. The realistic Hartree-Fock calculation thus supports the correspondence between nuclei and clusters suggested in Ref.[16] on the presence of the tetrahedron shell gap.

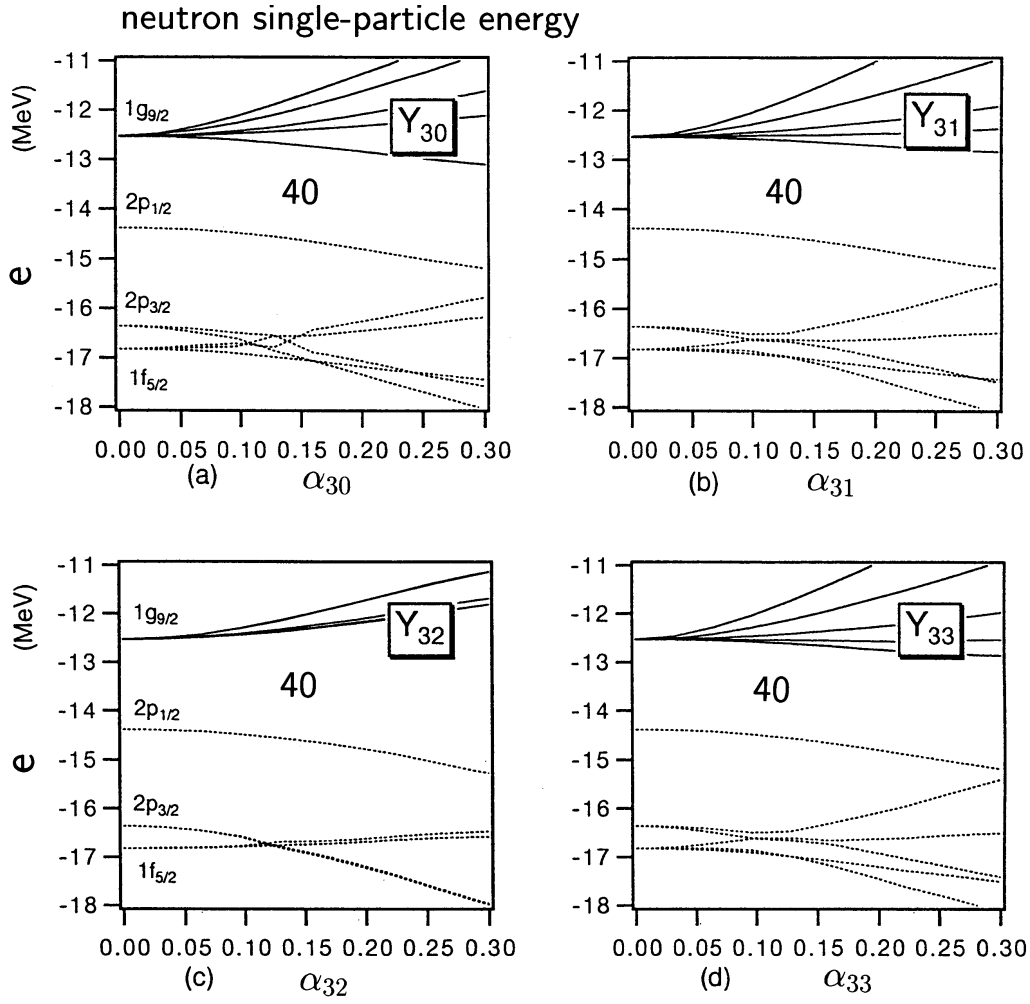

Figure 3: Neutron single-particle energies as a function of octupole deformation α_{3m} for $m = 0, 1, 2, 3$ ((a),(b),(c),(d), respectively) calculated for ^{80}Zr with $\beta = 0$. The quadrupole constraint is fixed to $\beta = 0$. The SIII force is used. The proton spectrum is almost the same as neutrons.

Triangular Softness in ^{68}Se

Concerning the oblate triangular solution of ^{68}Se, the minima is quite shallow with respect to the α_{33} direction. The energy gain due to the Y_{33} deformation (the energy difference between the minimum and the solution with $\beta_3, \alpha_{33} = 0$) is just 0.15 MeV. This indicates that the oblate state is extremely soft toward the α_{33} deformation rather than a rigid triangular deformation. It is noted that the potential energy curves for $\alpha_{3m} = 0 (m = 0, 1, 2)$ are not as soft as the α_{33} curve.

Systematics

In Fig.2 and Table 1 are seen systematic trends of the non-axial octupole deformations in $N = Z, A \sim 60 - 80$ nuclei. The octupole softness is enhanced at $N, Z \sim 34$, (representative is oblate ground state of ^{68}Se which is soft for triangular deformation), and at $N, Z \sim 40$ (the tetrahedral deformation). It is also seen that the Y_{33} mode is the softest among the four octupole deformations for the oblate states whereas Y_{31} and Y_{30} is favored for the prolate states. This is explained in terms of the single-particle shell structures near the Fermi surface[6]. For the oblate states, the high Ω orbits such as [404]9/2 and [413]7/2 stemming from $g_{9/2}$ are located near the Fermi surface of $N, Z \sim 34$ and strong Y_{33} coupling with [301]3/2 and [310]1/2 orbits emerges. On the other hand the $g_{9/2}$ low Ω orbits are situated far above the Fermi surface. Thus Y_{30} Y_{31} couplings are disfavored. For the prolate states Y_{31} is favored in a reversed reasoning. The Y_{32} deformations favored at $N, Z \sim 40$ is caused by the tetrahedron shell gap discussed above. The instability and the softness for the non-axial octupole deformations are quite contrasting with the axial octupole instability known in other mass regions.

5 Discussion

Sensitivity to force parameters

Besides SIII, other parameter sets such as SkM*[22] are known to provide a reasonable description of nuclear deformations. To check sensitivity to the force parameters we performed a calculation using SkM*. The calculated potential energy curves associated with an oblate HF solution in ^{68}Se and a spherical HF solution in ^{80}Zr are shown in Fig.4 (a) and (c). Although they do not have a minima at finite α_{3m}, the potential curve shows softness for the tetrahedral α_{32} direction of the ^{80}Zr spherical state ($\beta = 0$) and for the triangular α_{33} direction of the ^{68}Se oblate state. This qualitative agreement with the SIII results can be expected since the single-particle structures which play a central role for the mechanism for the non-axial octupole deformations are not very different for both parameter sets. In Fig.4(b) and (d), we show the results of SIII but with increased pairing force strength in order to show the sensitivity to the pairing correlation. Here we assumed 10% increase of $G_{n,p}$ which is within a reasonable range reproducing the experimental pairing gap (the odd-even mass difference). From comparison with Fig.2, it is seen that the pairing correlation have an effect to reduce the non-axial deformation. Note, however, that the essential features of the potential curve remain the same.

Spectral signatures

If a rigid tetrahedron deformation is realized, a characteristic pattern of excited spectra is expected. Rotational excitation of a even-even tetrahedron nucleus will accompany a sequence of levels $0^+, 3^-, 4^+, 6^+, 7^-, ...$ following the rotational energy relation $E(I) - E(0) = I(I + 1)/2\mathcal{J}$ in parallel with the tetrahedron molecule [26]. Here the spectrum is labeled by the irreducible representation of the T_d group. The rotational levels are connected by strong E3 transitions instead of E2. Viewing the potential energy curve for the tetrahedral solution in ^{80}Zr, we can expect not a rigid deformation but rather a transitional situation between the tetrahedron rotation and the octupole vibration around the spherical state. From the experimental systematics of the first 3^- excitation energy in the neighboring mass region [27], a typical octupole

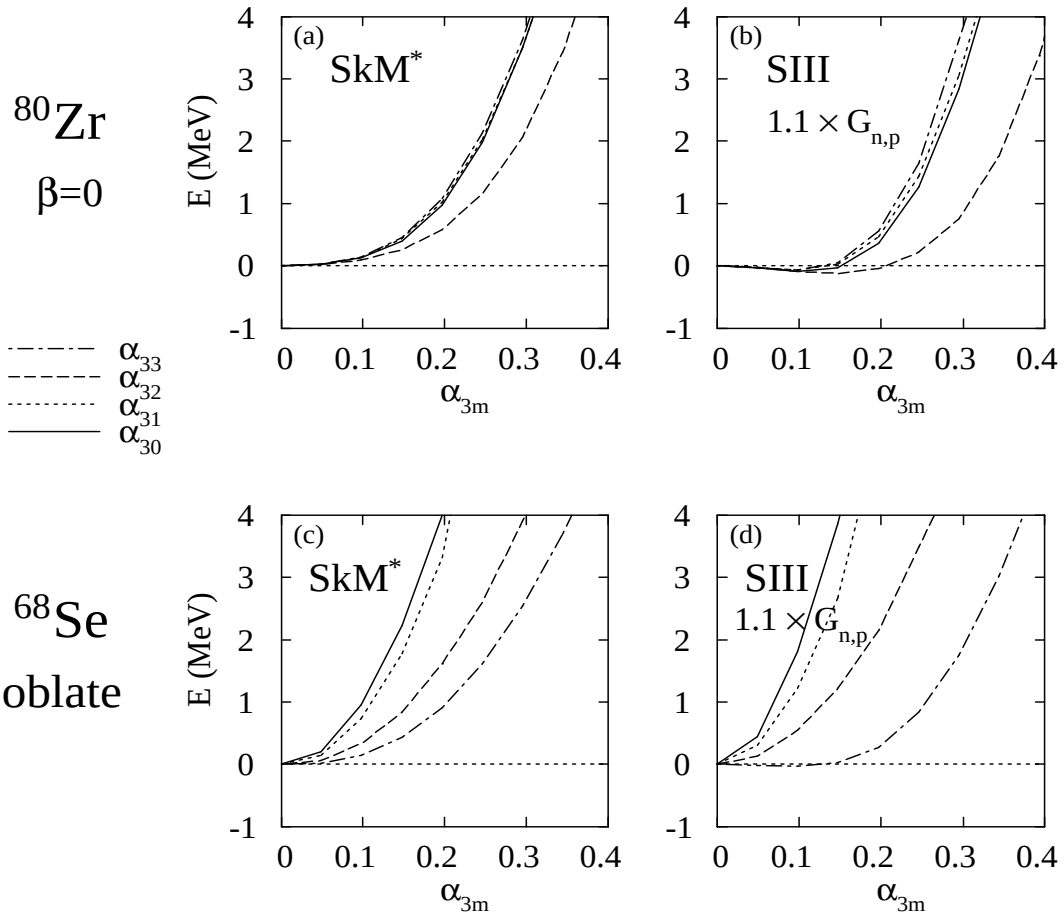

Figure 4: Potential energy curve calculated with the SkM* force (a,c), and with SIII and an increased pairing force $G_{n,p} = 18.15/(11 + N, Z)$ MeV (b,c), for the excited spherical state in ^{80}Zr (a,b) and the oblate state in ^{68}Se (c,d).

vibrational energy is about a few MeV. Using this estimate and the calculated potential energy curve for the α_{32} direction, amplitude associated with the transitional tetrahedral excitation is estimated to be about $\alpha_{32}(\beta_3) \sim 0.3$. This corresponds to $B(\mathrm{E3}) \sim 60$ W.u. on the basis of $B(\mathrm{E3}) = (3ZeR^3\beta_3/4\pi)^2$, which is much larger than the systematic values [28] in neighboring mass region.

For the oblate state in ^{68}Se, the potential energy curve suggests soft vibrational excitation for the Y_{33} direction which couples with the rotational excitation. We can expect for such case that the excitation spectra showing a $K^\pi = 0^+$ rotational band $(0^+, 2^+, 4^+, ..)$ associated with the ground state, and a $K^\pi = 3^-$ rotational band $(3^-, 4^-, 5^-, ..)$ associated with the vibrational excitation. From the calculated potential energy curve, the vibrational amplitude is estimated as $\alpha_{33}(\beta_3) \sim 0.2 - 0.3$, corresponding to $B(\mathrm{E3}) \sim 20 - 40$ W.u. for interband transitions.

The nuclei under discussion are close to the proton drip line, and experimental information on the excited spectra is not very rich at present. Candidates of negative parity states are found in ^{64}Ge, which suggests presence of some but not very strong octupole collectivity[24]. Quite recently candidate negative parity states are found in ^{68}Se, and the observed spectra looks similar to that in ^{64}Ge although the experimental information is not enough to see the octupole collectivity [25].

6 Conclusions

The fully three dimensional Hatree-Fock calculation suggests that the non-axial octupole deformations are important in $N = Z, A \sim 60 - 80$ nuclei. Prominent examples are the tetrahedral deformation of an shape coexisting excited state in ^{80}Zr, and the triangular softness of the oblate state in ^{68}Se. The tetrahedron deformation causes a shell gap at $N, Z = 40$, which founds the microscopic origin of the exotic shape.

References

[1] As a review, P. A. Butler and W. Nazarewicz, *Rev. Mod. Phys.* **68**, 349 (1996).

[2] As a review, Y. Fujiwara, H. Horiuchi, K. Ikeda, M. Kamimura, K. Katō, Y. Suzuki and E. Uegaki, *Prog. Theor. Phys. Suppl.* **68**, 29 (1980);
H. Horiuchi and K. Ikeda, in *International Review of Nuclear Physics*, ed. T. T. S. Kuo and E. Osnes (World Scientific, Singapore, 1986), Vol. 4, p. 1.

[3] X. Li and J. Dudek, *Phys. Rev.* **C94**, R1250 (1994).

[4] X. Li, J. Dudek, and P. Romain, *Phys. Lett.***B271**, 281 (1991).

[5] R. R. Chasman, *Phys. Lett.* **B266**, 243 (1991).

[6] S. Takami, K. Yabana and M. Matsuo, *Phys. Lett.* **B431**, 242 (1998).

[7] J. Skalski, *Phys. Rev.* **C43**, 140 (1991).

[8] As a review, J.L. Wood, K. Heyde, W. Nazarewicz, M. Huyse and P. Van Duppen *Phys. Rep.* **215**, 101 (1992).

[9] C.J.Lister, M.Campbell, A.A.Chishti, W.Gelletly, L.Goettig, R.Moscrop, B.J.Vary, A.N.James, T.Morrison, H.G.Price, J.Simpson, K.Connel, and O.Skeppstedt, *Phys. Rev. Lett.* **59**, 1270 (1987);
B.J.Vary, M.Campbell, A.A.Chishti, W.Gelletly, L.Goettig, C.J.Lister, A.N.James, and O.Skeppstedt, *Phys. Lett.* **B194**, 463 (1987);
H.Dejbakhsh, T.M.Cormier, X.Zhao, A.V.Ramayya, L.Chaturvedi, S.Zhu, J. Kormicki, *Phys. Lett.* **B249**, 195 (1990);
Kr C.J.Lister, P.J. Ennis, A.A. Chishti, B.J.Varley, W.Gelletly, H.G. Price, A.N. James, *Phys. Rev.* **C42**, R1191 (1990);
W. Gelletly, M.A. Bentley, H.G. Price, J.Simpson, C.J. Gross, J.L. Durell, B.J. Varley, O.Skeppstedt and S. Rastikerdar, *Phys. Lett.* **B253**, 287 (1991);
G.de Angelis, C.Fahlander, A.Gadea, E.Farnea, W.Gelletly, A.Aprahamian, D.Bazacco, F.Becker, P.G.Bizzeti, A.Bizzeti-Sona, F.Brandolini, D.de Acuña, M. De Poli, J. Eberth, D. Foltescu, S.M.Lenzi, S.Lunardi, T.Martinez, D.R.Napoli, P.Pavan, C.M.Petrache, C.Rossi Alvarez, D.Rudolph, B.Rubio, W.Satuła, S.Skoda, P.Spolaore, H.G.Thomas, C.A. Ur, and R.Wyss, *Phys. Lett.* **B415**, 217 (1997).

[10] W. Nazarewicz, P. Olanders, I. Ragnarsson, J. Dudek, G. A. Leander, P. Mőller and E. Ruchowska, *Nucl. Phys.* **A429**, 269 (1984).

[11] G. A. Leander, R. K. Sheline, P. Mőller, P. Olanders, I. Ragnarsson and A. J. Sierk, *Nucl. Phys.* **A388**, 452 (1982).

[12] W.A. de Heer, *Rev. Mod. Phys.* **65**, 611 (1993);
M. Brack, *Rev. Mod. Phys.* **65**, 677 (1993).

[13] I. Hamamoto, B. Mottelson, H. Xie and X. Z. Zhang, *Z. Phys.* **D21**, 163 (1991).

[14] F. Frisk, I. Hamamoto and F. R. May, *Phys. Scr.* **50**, 628 (1994).

[15] S.M. Reimann, M. Koskinen, H. Häkkinen, P.E. Lindelof, and M. Manninen, *Phys. Rev.* **B56**, 12147 (1997).

[16] J. Kolehmainen, M. Koskinen, H. Häkkinen, M. Manninen, and S. Reimann, *Czech. J. Phys.* **48**, 679 (1998).

[17] P. Bonche, H. Flocard, P.-H. Heenen, S. J. Krieger and M. S. Weiss, *Nucl. Phys.* **A443**, 39 (1985).

[18] N. Tajima, S. Takahara and N. Onishi, *Nucl. Phys.* **A603**, 23 (1996).

[19] K. T. R. Davies, H. Flocard, S. Krieger and M. S. Weiss, *Nucl. Phys.* **A342**, 111 (1980).

[20] S. Takami, K. Yabana and K. Ikeda, *Prog. Theor. Phys.* **96**, 407 (1996);
S. Takami, K. Yabana and K. Ikeda, *Proc. XVII RCNP Int. Symp. on Innovative Computational Methods in Nuclear Many-Body Problems*, ed. H.Horiuchi, M.Kamimura, H.Toki, Y.Fujiwara, M.Matsuo and Y.Sakuragi (World Scientific, Singapore, 1998) pp.112-116.

[21] M. Beiner, H.Flocard, Nguen Van Giai and P. Quentin, *Nucl. Phys.* **A238**, 29 (1975).

[22] J. Bartel, P. Quentin, M. Brack, C. Guet and H.-B. Håkansson, *Nucl. Phys.* **A386**, 79 (1982).

[23] P.-H.Heenen, J.Skalski, P. Bonche, and H. Flocard, *Phys. Rev.* **C50**, 802 (1994).

[24] P. J. Ennis, C. J. Lister, W. Gelletly, H. G. Price, B. J. Varley, P. A. Butler, T. Hoare, S. Cwiok and W. Nazarewicz, *Nucl. Phys.* **A535**, 392 (1991).

[25] S. Skoda, B.Fielder, F.Becker, J. Eberth, S.Freund, T.Steinhardt, O.Stuch, O. Thelen, H.G. Thomas, L. Käubler, J. Reif, H.Shnare, R.Schwengner, T.Servene, G.Winter,V.Fischer, A.Jungclaus, D.Kast, K.P.Lieb, C.Teich, C,Ender, T.Hä rtlein, F.Köck, D.Schwarlm and P.Baumann, *Phys. Rev.* **C58**, R5 (1998).

[26] G. Herzberg, *Molecular Spectra and Molecular Structure* Vol. II (D. Van Nostrand Company, New York, 1945).

[27] P.D. Cottle, *Phys. Rev.* **C42**, 1264 (1990).

[28] R.H. Spear and W.N. Catford, *Phys. Rev.* **C41**, R1351 (1990).